TRANSACTIONS ON ELECTRICAL AND ELECTRONIC MATERIALS
Vol. 14, No. 4, pp. 216-220, August 25, 2013

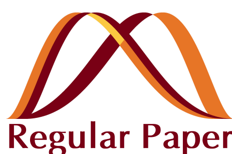

pISSN: 1229-7607 eISSN: 2092-7592
DOI: http://dx.doi.org/10.4313/TEEM.2013.14.4.216

Dry Etching Characteristics of Indium Zinc Oxide Thin Films in Adaptive Coupled Plasma

Jong-Chang Woo and Chang-Auck Choi
Nano Convergence Sensor Research Section, Electronics and Telecommunications Research Institute, Daejeon 305-700, Korea

Chang-Il Kim†
School of Electrical and Electronics Engineering, Chung-Ang University, Seoul 156-756, Korea

Received May 20, 2013; Revised June 3, 2013; Accepted July 3, 2013

The etching characteristics of indium zinc oxide (IZO) in Cl_2/Ar plasma were investigated, including the etch rate and selectivity of IZO. The IZO etch rate showed non-monotonic behavior with increasing Cl_2 fraction in the Cl_2/Ar plasma, and with increasing source power, bias power, and process pressure. In the Cl_2/Ar (75:25%) gas mixture, a maximum IZO etch rate of 87.6 nm/min and etch selectivity of 1.09 for IZO to SiO_2 were obtained. Owing to the relatively low volatility of the by-products formation, ion bombardment was required, in addition to physical sputtering, to obtain high IZO etch rates. The chemical state of the etched surfaces was investigated with X-ray photoelectron spectroscopy. These data suggested that the IZO etch mechanism was ion-enhanced chemical etching.

Keywords: Etching, Indium zinc oxide, IZO, X-ray photoelectron spectroscopy, Cl_2

1. INTRODUCTION

Indium zinc oxide (IZO), a wide band gap transparent conducting oxide, has drawn considerable interest recently, because of its many potential applications, including transparent conducting electrodes, optoelectronics, photonics, and sensors. These devices can be fabricated under low-voltage operations, and the designing of such devices will pave the way for the next generation of display technologies based on transparent and flexible devices. IZO thin films have attracted a great deal of attention, because of their excellent optical transmission, high conductivity, chemical stability, thermal stability, and low compressive stress. Of the various patterning techniques for IZO thin films, plasma etching is preferred, because it allows high-resolution pattern transfer for optoelectronic device structures [1-3].

† Author to whom all correspondence should be addressed:
E-mail: cikim@cau.ac.kr

Copyright ©2013 KIEEME. All rights reserved.
This is an open-access article distributed under the terms of the Creative Commons Attribution Non-Commercial License (http://creativecommons.org/licenses/by-nc/3.0) which permits unrestricted noncommercial use, distribution, and reproduction in any medium, provided the original work is properly cited.

Recently, the deposition process of IZO thin films has been extensively studied, and various deposition methods, including chemical vapor deposition, sputtering, and sol-gel, have been reported [4,5]. While the growth characteristics of IZO thin films are relatively well optimized, an efficient pattern transfer process remains to be developed. Among the various patterning techniques, dry etching processing has advantages over conventional wet etching processes, including high resolution and easy process automation.

Research to date shows the dependence of the IZO etch rate on the operating conditions using Cl_2/Ar, Ar/CH_4/H_2, C_2F_6/Ar, IBr, and BI_3 plasmas, but it does not discuss the etch mechanism, the relationships between the process parameters, or the chemistry [6-8]. Only a few studies examined IZO dry etching using the adaptive coupled plasma sources favored by modern microelectronic technology. As a result, the effect of the process parameters on the IZO etch rate has not been explored in detail, and the IZO etch mechanism is not quite clear.

In this work, we investigated the etching characteristics of IZO thin films using Cl_2/Ar mixtures in an adaptive coupled plasma (ACP) system. The chemical reactions on the surface of the etched IZO thin films were investigated by X-ray photoelectron

spectroscopy (XPS). Field emission Auger electron spectroscopy (FE-AES) was used for the elemental analysis of the etched surfaces. The etch rate for the patterns of the IZO thin film was measured using field emission scanning electron microscopy (FE-SEM).

2. EXPERIMENTAL DETAILS

IZO thin films were prepared on a Si (100) substrate, using a traveling-wave-type atomic layer deposition (ALD) reactor (Evertek, Plus-100). The deposition temperature of the IZO films was 15℃, and their final thickness was about 120 nm. The etching experiments were performed in a planar ACP system (Selex 200, APTC Co.) [9]. As shown in Fig. 1, the system consists of multi-spiral coils and a bushing, and the coil antenna was located above a thick horizontal ceramic window. A 12.56-MHz RF power generator was connected to the coil antenna to generate the plasma. Another 13.56-MHz RF power generator was connected to the electrostatic chuck (ESC), to control the ion energy [10,11]. This plasma source shows characteristics of both traditional sources of inductively coupled plasma and capacitively coupled plasma, as well as its own characteristics. The etching of the IZO thin film was studied as a function of the Cl_2 content in the Cl_2/Ar plasma. The gas mix ratio and process pressure were varied, to determine the etching characteristics. For these experiments, the source power, bias power, process pressure, and substrate temperature were 400 W, 100 W, 1.3 Pa and 45℃, respectively. The etch rate was measured by surface profiler (KLA Tencor, α-step 300). The chemical reactions on the surface of the etched IZO thin films were investigated by XPS (SIGMA PROBE, Thermo VG), with Mg K_{α}(1,253.6 eV) radiation at 300 W. The narrow-scan spectra of all of the regions of interest were recorded with pass energy of 5 - 320 eV, to quantify the surface composition, and identify the chemical binding state. All of the XPS samples were bare IZO thin films 1 cm × 1 cm in size, without any photo-resist (PR) patterns. During these measurements, the X-ray power was 220 W at 11.1 mA. Using a pass energy of 25 eV, a spectral resolution of 0.45 eV was obtained. FE-AES (Microlab 310-D, Thermo VG Scientific) used for the elemental analysis of the etched samples is a surface-sensitive spectroscopic technique. The IZO thin films used for the measurement of the etch rate and cross section were characterized using FE-SEM (Sirion 400, FEI). The width and thickness of the PR patterns were 1.5 and 1.02 μm, respectively.

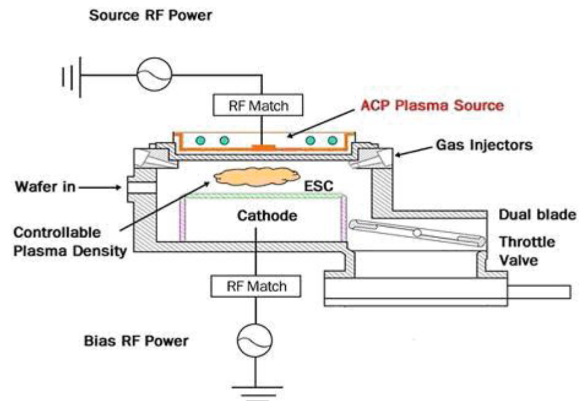

Fig. 1. Schematic diagram of the adaptively coupled plasma system.

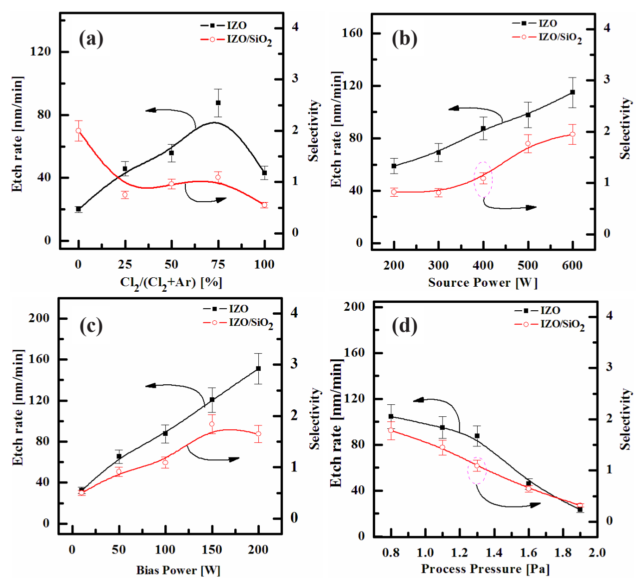

Fig. 2. The etch rate of IZO thin film and the selectivity of IZO to SiO_2 as a function of (a) Cl_2/Ar gas mixing ratio, (b) source power, (c) bias power, and (d) process pressure.

3. RESULTS AND DISCUSSION

3.1 The effect of the etch characterization in the ACP system

For the etch characterization of the IZO thin film in the ACP system, the etch characteristics of the IZO thin film were systematically investigated as a function of the Cl_2/Ar gas mixing ratio, source power, bias power, and process pressure. Figure 2(a) shows the etch rate of the IZO thin film, and its selectivity to SiO_2 as a function of the Cl_2/Ar mixing ratio, at a process pressure of 1.3 Pa, source power of 400 W, and bias power of 100 W. As the Cl_2 content in the Cl_2/Ar plasma increased, the IZO thin film etch rate also increased, and reached a maximum of 87.6 nm/min at a Cl_2/Ar (75:25%) gas mixture. The etch rates of IZO in pure Ar and pure Cl_2 were 20 and 43.2 nm/min, respectively. This suggests that for a given range of experimental conditions, the chemical etching pathway is more effective than the physical one. As the Cl_2 content in the Cl_2/Ar plasma increased from 0 to 75%, the selectivity of IZO to SiO_2 decreased from 2 to 0.55, respectively. There are several possible explanations for the dominance of the chemical etching pathway. One is the volatility of the compounds, given that the melting points for InCl, $InCl_2$, $InCl_3$, and $ZnCl_2$ are about 211, 235, 583, and 290℃, which allow the Cl atoms that form in the plasma to spontaneously react with the IZO compounds. Another possible reason is that ion bombardment, which breaks the oxide bonds, is required for the chemical reactions. As the Cl_2 content was increased in the Cl_2/Ar plasma, the bias voltage was also increased at a fixed bias power [12]. Figure 2(b) shows the etch rate of the IZO thin film and the etch selectivity of IZO to SiO_2 as a function of the source power, for the Cl_2/Ar (75:25%) plasma. As the source power increased from 200 W to 600 W, the IZO etch rate increased from 58.8 nm/min to 115 nm/min, while the selectivity of IZO to SiO_2 increased from 0.82 to 1.95, respectively. This result is related to the variation in the dependence of the etch rate on the material. Such behavior of all of the etch rates with increasing source power can be explained by the acceleration of both the physical and chemical etching pathways, through the increase of the dissociation rate, as well as ionization rates, due to the increased source power, and the

volume densities and fluxes of chlorine atoms, Cl radicals and positive ions increased as the results. Figure 2(c) shows the etch rate of the IZO thin films and the etch selectivity of IZO to SiO_2, as a function of the bias power for the Cl_2/Ar (75:25%) plasma. As the bias power increased from 10 to 200 W, the etch rate increased from 32.5 to 151 nm/min, while the selectivity of IZO to SiO_2 increased linearly. This result is also related to the variation in etch rate dependent on the material. In general, the induced self-bias voltage to the wafer increases with the increasing bias power. The etch rate will be increased with high bias voltage in reactive ion etching mechanism. However, in our experiment, we obtained a decreasing tendency of the IZO etch rate with increasing bias power. Therefore, it is not the reactive ion etching mechanism, and the increase in the etch rate is thought to be associated with the increase in the mean ion energy, resulting in an increase in the sputtering yields for both IZO and the reaction products. This can be explained by the adsorbed Cl_x radical and C atoms being removed, before the chemical reaction with IZO film, at the high bias power [12]. Figure 2(d) shows the etch rate of the IZO thin film, and its selectivity to SiO_2 as a function of the process pressure for a Cl_2/Ar (75:25%) gas mixture. As the process pressure increased from 0.8 to 1.9 Pa, the IZO etch rate decreased from 104.8 to 23.4 nm/min, while the selectivity of IZO to SiO_2 decreased from 1.78 to 0.32, respectively. This result is also related to the variation in the etch rate dependent on the material. We consider that the effect of the process pressure is as follows. An increase in the process pressure enhances the density of the neutral chemically active species, but lowers the ion mean free path and ion energy. Even if the mean ion energy and the sputtering yield were decreased, we achieved higher etch rate at high pressure. This effect can be explained by the fact that it needs some residency time for etchant in IZO etching with Cl_2/Ar plasma. When the pressure is low, the etchant is easily evacuated without chemical reaction with the IZO thin film. However, the etchant can reside for high pressure, and the chemical reaction time is sufficient to form etch by-products. As a result of the effect of the process pressure on the IZO etch rate and the volume densities of Cl atoms and radicals, the etch rate of the IZO thin films is decreased, because of the decreasing physical effects.

3.2 XPS analysis

The chemical states of the etched surfaces of the IZO thin films were investigated by XPS analysis. Figure 3 shows the XPS narrow-scan spectra for In $3d_{5/2}$ taken at a 90° angle. These spectra of the IZO film surface were taken before and after etching in pure Cl_2 and a Cl_2/Ar (75:25%) gas mixture. The peaks obtained from the as-deposited IZO film were used as a reference. The peak at 445.25 eV corresponds to the In $3d_{5/2}$ bond. When the IZO thin films were exposed to the Cl_2/Ar (75:25%) plasma and the pure Cl_2 plasma, the core peak of In $3d_{5/2}$ was shifted from 445.85 eV to a higher binding energy of 446.45 eV and 446.25 eV. As shown in Fig. 3(a), a chemical shift occurred in the plasma, but the shape of the In 3d peak was broadened. For the as-deposited film, as shown in Fig. 3(b), the In $3d_{5/2}$ peak can be decomposed into two peaks corresponding to the In-Metal bond (444.9 eV) and In-O bond (446.7 eV). The intensity of this peak decreased with increasing Cl_2 and Ar mixing ratio, as shown in Figs. 3(c)-(d), and the In $3d_{5/2}$ peak can be decomposed into three peaks corresponding to the In-Metal bond (the same as 444.9 eV) and In-O bond (the same as 446.7 eV), and we can therefore associate it with the signal from In-Cl_x (445.7 eV). The etching processes in the Cl_2/Ar (75:25%) plasma and pure Cl_2 plasma caused a noticeable decrease in the In $3d_{5/2}$ peak, which can be attributed to the destruction of the oxide bonds by ion bombardment. This chemical shift indicated that a chemical reaction occurred between In and Cl, resulting in the formation of In-Cl bonds on the surface [13].

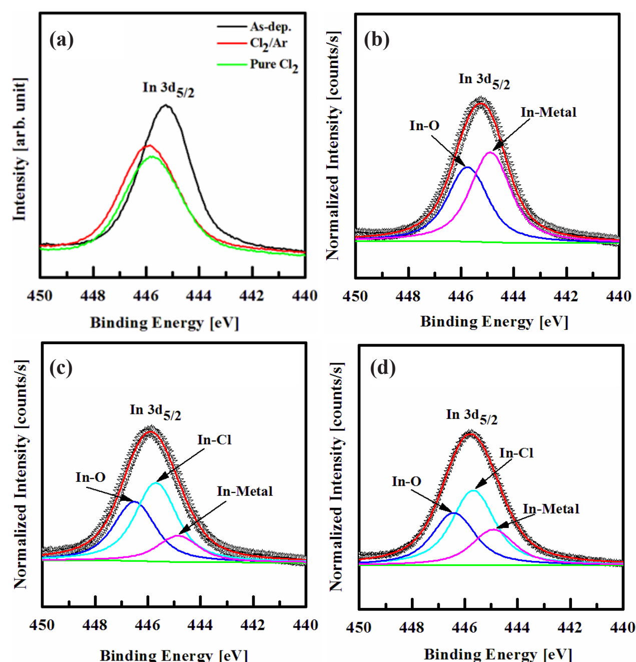

Fig. 3. The In $3d_{5/2}$ XPS spectra with peak deconvolution results on the surface of the etched IZO thin films as a function of gas mixing ratio. (a) Narrow-scan spectra, (b) As-deposited, (c) Cl_2/Ar (75:25%), and (d) pure Cl_2.

Figure 4 shows the XPS narrow-scan spectra for Zn $2p_{3/2}$ taken at a 90° angle. These spectra of the IZO film surface were taken before and after etching in pure Cl_2 and a Cl_2/Ar (75:25%) gas mixture. The peaks obtained from the as-deposited IZO film were used as a reference. The peak at 1021.9 eV corresponds to the Zn $2p_{3/2}$ bond. When the IZO thin film was exposed to the Cl_2/Ar (75:25%) plasma and the pure Cl_2 plasma, the core peak of Zn $2p_{3/2}$ was shifted to a higher binding energy of 1024.1 eV and 1023.95 eV. As shown in Fig. 4(a), a few chemical shifts occurred in the plasma, but the shape of the Zn $2p_{3/2}$ peak was broadened. For the as-deposited film, as shown in Fig. 4(b), the Zn $2p_{3/2}$ peak can be decomposed into two peaks, corresponding to the Zn-O bond (1021.64 eV) and Zn-Zn bond (1022.54 eV). As shown in Figs. 4 (c)-(d), the Zn $2p_{3/2}$ peak can be decomposed into three peaks, corresponding to the Zn-O bond (1022.49 eV, 1021.69 eV) and Zn-Zn bond (1024.3 eV, 1023.45 eV); and the etching process in the Cl_2/Ar (75:25%) plasma in the Zn-Cl bond (1023.3 eV) and pure Cl_2 plasma causes a noticeable decrease in the Zn-Cl bond (1022.54 eV) peak, which can be attributed to the destruction of the oxide bonds by ion bombardment. This chemical shift indicates that a chemical reaction occurred between Zn and Cl, resulting in the formation of Zn-Cl bonds on the surface [14].

Figure 5 shows the XPS narrow-scan spectra for O 1s taken at a 90° angle. These spectra of the IZO film surface were taken before and after etching in pure Cl_2 and a Cl_2/Ar (75:25%) gas mixture. The peaks obtained from the as-deposited IZO film were used as a reference. The peak at 531.55 eV corresponds to the O 1s bond. When the IZO thin film was exposed to the Cl_2/Ar (75:25%) plasma and the pure Cl_2 plasma, the core peak of O 1s was moved to a higher binding energy of 533.55 eV and 533.1 eV. As shown in Fig. 5(a), a few chemical shifts occurred in the plasma, but the shape of the O 1s peak was broadened. For the as-deposited film, as shown in Fig. 5(b), the O 1s peak can be decomposed into three peaks, corresponding to the O-

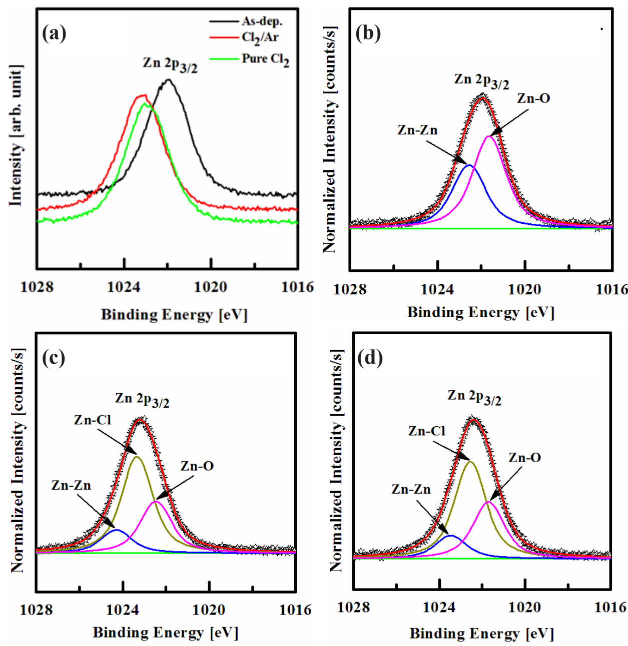

Fig. 4. The Zn $2p_{3/2}$ XPS spectra with peak deconvolution results on the surface of the etched IZO thin films as a function of gas mixing ratio. (a) Narrow-scan spectra, (b) As-deposited, (c) Cl_2/Ar (75:25%), and (d) pure Cl_2.

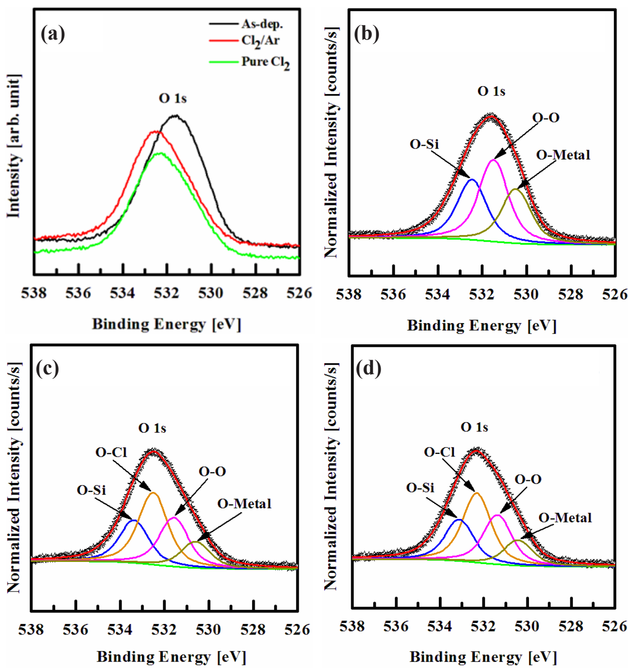

Fig. 5. The O 1s XPS spectra with peak deconvolution results on the surface of the etched IZO thin films as a function of gas mixing ratio. (a) Narrow-scan spectra, (b) As-deposited, (c) Cl_2/Ar (75:25%), and (d) pure Cl_2.

Metal (530.45 eV), O-O (531.5 eV) and O-Si (532.45 eV) bonds. As shown in Figs. 5(c)-(d) for O 1s, the O 1s peak can be decomposed into four peaks, corresponding to the O-Metal (530.6 eV, 530.4 eV), O-O (531.5 eV, 531.35 eV) and O-Si (533.4 eV, 533.15 eV) bonds; and after etching the IZO thin film in the plasma, the shoulder peak of O-Cl (532.5 eV) decreased significantly, and the

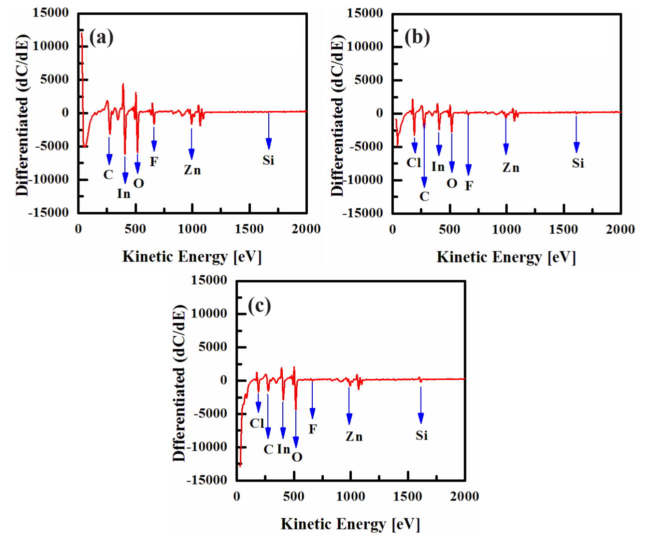

Fig. 6. AES analysis of the IZO surface, after etching in Cl_2/Ar plasma using different gas mixtures: (a) As-deposited, (b) Cl_2/Ar (75:25%), and (c) pure Cl_2.

core O 1s peak at 531.55 eV was shifted to 532.55 eV, as a result of the preferential removal of the adsorbed molecules. However, in the spectra of the IZO thin films that were etched in the Cl_2/Ar (75:25%) and pure Cl_2 plasmas, the O 1s peak intensities corresponding to the O-Metal (530.7 eV), O-O (531.5 eV), O-Cl (532.5 eV) and O-Si (535.5 eV) bonds decreased, owing to the formation of O-Cl bonds [15]. The intensity of the O 1s peak for the IZO thin films etched in Cl_2/Ar plasma is higher than that for the film etched in the pure Cl_2 plasma, which demonstrates that there was a dramatic increase in the number of O-Cl bonds, such as Cl_2O_3, owing to the dissociation of the In-Zn-O bonds by the ion bombardment. It is also possible that O-Cl bonds were formed, although this was not demonstrated here. The XPS results reveal that In, Zn, and O were removed by chemical reactions with Cl radicals, and by the physical bombardment of Ar ions [16].

3.3 AES analysis

To investigate the chemical states, the as-deposited IZO thin film was used as a reference, and compared with the etched IZO surfaces. Figure 6 shows the raw AES data that were acquired from the IZO surfaces of the as-deposited IZO thin film, and the film etched in the Cl_2/Ar (75:25%) and pure Cl_2 plasmas. As shown in Fig. 6, the components of IZO (In, Zn, O), under layer (Si) and carbon adsorbed from the air were detected. The etching time was 10 sec. The surfaces of all of the samples were contaminated with carbon and oxygen, owing to their exposure to the air, as shown in Fig. 6(a). Small amounts of F were detected in the fluorine coating, after etching in the plasma. No F element was detected on the etched surface, owing to the limited sensitivity of the FE-AES equipment. The existence of F element in the FE-AES analysis was confirmed by the detection of titanium chlorine bonds in the XPS analysis [15]. In Fig. 6(b), after etching in the Cl_2/Ar plasma, the intensities for In, Zn, and O were decreased, and those for Cl were increased. This indicates that the IZO thin film chemically reacted with Cl from the $C1_2$/Ar plasma, and that Cl was removed from the surface. This means that more Cl atoms remained in the surface reaction layer for the film etched by Cl_2/Ar plasma than that by pure Cl_2 plasma. The increase of the O peaks is due to the fact that the adsorbed C has a high chemical reaction energy which attracts O from the atmosphere when the

sample is exposed to air for the measurement. In Fig. 6(c), we obtained a high accumulation of C peaks, which is reduced by the plasma etching on the IZO surfaces. Therefore, weak intensities were observed for the In, Zn and O peaks.

4. CONCLUSIONS

In this work, we experimentally investigated the indium zinc oxide (IZO) etching mechanism in Cl_2/Ar plasma. We found that increasing the Cl_2 content in the Cl_2/Ar plasma leads to an increase in the IZO etch rate, up to a maximum value of 87.6 nm/min at a concentration of 75% Cl_2. This suggests that the mean ion energy decreased, while the ion current and Cl atom flux should increase. So, it is hard to conclude with the physical effects increasing due to the relatively low volatility of the by-products formed during Cl_2/Ar plasma etching, that ion bombardment was required, in addition to physical sputtering, to obtain these high IZO etch rates. The reason for the existence of a maximum etch rate was found to be the concurrence of both physical and chemical pathways in the ion-assisted chemical reaction. The volatile oxygen compounds identified by XPS suggests that the composition of the sample etched in the Cl_2/Ar plasma was identical to that of the as-deposited sample. These tendencies were very similar to the etch characteristics. This result is in agreement with the universal energy dependence of the ion-enhanced chemical etching yield.

ACKNOWLEDGMENT

This research was conducted under the industrial infrastructure program for fundamental technologies (N0000417), which is funded by the Ministry of Knowledge Economy(MOTIE, Korea). [The Construction of Foundry Base Technology for The Smart Micro-Sensor Commercialization (N0000417)].

REFERENCES

[1] W. S. Cheong, J. M. Lee, J. H. Lee, S. H. Park, S. M. Yoon, C. W. Byun, S. H. Yang, S. M. Chung, K. I. Cho, C. S. Hwang, ETRI Journal 31 (2009) 660 [DOI: http://dx.doi.org/10.4218/etrij.09.1209.0049].

[2] N. Ito, Y. Sato, P. K. Song, A. Kaijio. , K. Inoue, Y. Shigesato, Thin Solid Films 496 (2006) 99 [DOI: http://dx.doi.org/10.1016/j.tsf.2005.08.257].

[3] S. H. Park, D. H. Cho, C. S. Hwang, S. H. Yang, M. K. Ryu, C. W. Byun, S. M. Yoon, W. S. Cheong, K. I. Cho, J. H. Jeon, ETRI Journal 31 (2009) 653 [DOI: http://dx.doi.org/10.4218/etrij.09.1209.0043].

[4] K. Tominaga, T. Takao, A. Fukushima, T. Moriga, I. Nakabayashi, Vacuum 66 (2002) 505 [DOI: http://dx.doi.org/10.1016/S0042-207X(02)00123-9].

[5] S. Y. Lee, B. O. Park, Thin Solid Films 484 (2005) 184 [DOI: http://dx.doi.org/10.1016/j.tsf.2005.03.007].

[6] W. T. Lim, L. Stafford, J. I. Song, J. S. Park, Y. W. Heo, J. H. Lee, J. J. Kim, S. J. Pearton, Appl. Surf. Sci. 253 (2007) 3773 [DOI: http://dx.doi.org/10.1016/j.apsusc.2006.07.094].

[7] W. T. Lim, L. Stafford, J. S. Wright, L. F. Vossa, R. Khanna, J. I. Song, J. S. Park, Y. W. Heo, J. H. Lee, J. J. Kim, D. P. Norton, S. J. Pearton, Appl. Surf. Sci. 253 (2007) 9228 [DOI: http://dx.doi.org/10.1016/j.apsusc.2007.05.061].

[8] L. Stafford, W. T. Lim, S.J. Pearton, M. Chicoine, S. Gujrathi, F. Schiettekatte, J. S. Park, J. I. Song, Y. W. Heo, J. H. Lee, J. J. Kim, I. I. Kravchenko, J. Vac. Sci. Technol. A 25 (2007) 659 [DOI: http://dx.doi.org/10.1116/1.2736679].

[9] J. C. Woo, S. G. Kim, J. G. Koo, G. H. Kim, D. P. Kim, C. H. Yu, J. Y. Kang, C. I. Kim, Thin Solid Films 517 (2009) 4246. [DOI: http://dx.doi.org/10.1016/j.tsf.2009.02.012]

[10] W. U. Chung, S. R. Oh, J. H. You, K. T. Lim, Y. K. Oh, N. H. Kim, Proceedings of 13th Korean Conference on Semiconductor, 2006 Feb 23-24, Jeju, Korea: (2006) 909.

[11] N. H. Kim, inventor: APTC Co, assignee. Adaptively coupled plasma source having uniform magnetic field distribution and plasma chamber having the same. United States Patent US2009015635. Jun 18, 2009.

[12] D. P. Kim, K. T. Kim, C. I. Kim, A. M. Efremov, Thin Solid Films 447-448 (2004) 343 [DOI: http://dx.doi.org/10.1016/S0040-6090(03)01115-5].

[13] T. Ishida, H. Kobayashi, Y. Nakato, J. Appl. Phys. 73 (1993) 4344 [DOI: http://dx.doi.org/10.1063/1.352818].

[14] B. Kumar, H. Gong, R. Akkipeddi, J. Appl. Phys. 97 (2005) 063706 [DOI: http://dx.doi.org/10.1063/1.1862311].

[15] J. F. Moulder, W. F. Stickle, P. E. Sobol, K. D. Bomben, Handbook of X-ray Photoelectron Spectroscopy, Physical Electronics, Inc. 1995.

[16] G. Prumper, X. J. Liu, K. Ueda, and Y. Tamenori, Radiat. Phys. Chem. 75 (2006) 2019 [DOI: http://dx.doi.org/10.1016/j.radphyschem.2005.11.020].